

Synthetic analogues of the parasitic worm product, ES-62 reduce disease development in *in vivo* models of fibrosis

Colin J. Suckling^a, Sambuddho Mukherjee^b, Abedawn I. Khalaf^a, Ashwini Narayan^b, Fraser J. Scott^a, Sonal Khare^b, Saravanakumar Dhakshinamoorthy^b, Margaret M. Harnett^c and William Harnett^{d*}

^aDepartment of Pure & Applied Chemistry, University of Strathclyde, Glasgow G1 1XL, UK

^bDepartment of Discovery Biology, Jubilant Biosys Ltd, Bangalore-560022, India

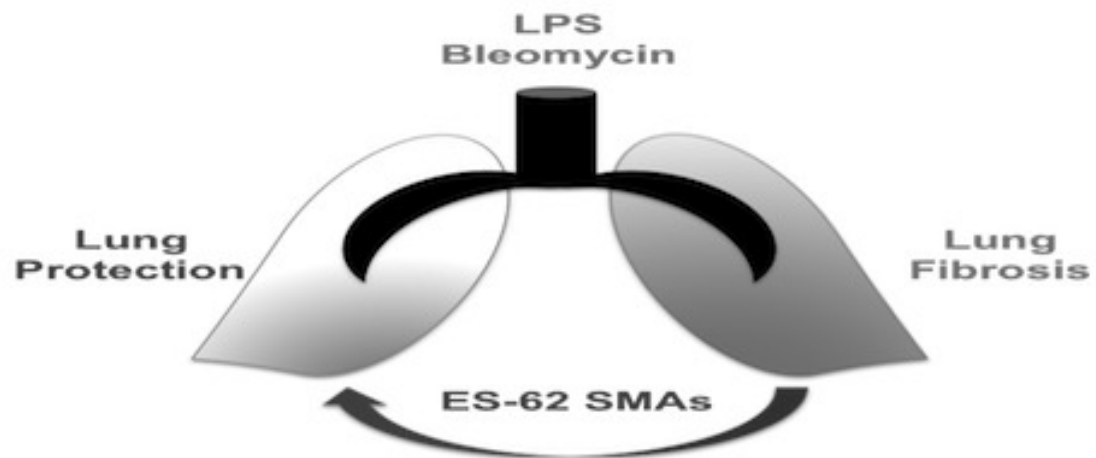
^cInstitute of Infection, Immunity and Inflammation, University of Glasgow, Glasgow G12 8TA, UK

^dStrathclyde Institute of Pharmacy and Biomedical Sciences (SIPBS), University of Strathclyde, Glasgow G4 0RE

*Corresponding Author: Prof. William Harnett, SIPBS, 161 Cathedral Street, University of Strathclyde, Glasgow G4 0RE, UK; e.mail: w.harnett@strath.ac.uk; phone: (0044)-141-548-3725

Summary

Synthetic small molecule analogues (SMAs) of ES-62, an immunomodulator secreted by the filarial nematode *Acanthocheilonema viteae* protect against LPS- and Bleomycin-induced lung fibrosis in mice.



1 **Synthetic analogues of the parasitic worm product ES-62, reduce disease**
2 **development in *in vivo* models of lung fibrosis**

3

4 Colin J. Suckling^a, Sambuddho Mukherjee^b, Abedawn I. Khalaf^a, Ashwini Narayan^b,
5 Fraser J. Scott^a, Sonal Khare^b, Saravanakumar Dhakshinamoorthy^b, Margaret M.
6 Harnett^c and William Harnett^{d*}

7

8 ^aDepartment of Pure & Applied Chemistry, University of Strathclyde, Glasgow G1 1XL,
9 UK

10 ^bDepartment of Discovery Biology, Jubilant Biosys Ltd, Bangalore-560022, India

11 ^cInstitute of Infection, Immunity and Inflammation, University of Glasgow, Glasgow G12
12 8TA, UK

13 ^dStrathclyde Institute of Pharmacy and Biomedical Sciences (SIPBS), University of
14 Strathclyde, Glasgow G4 0RE

15 *Corresponding Author: Prof. William Harnett, SIPBS, 161 Cathedral Street, University
16 of Strathclyde, Glasgow G4 0RE, UK; e.mail: w.harnett@strath.ac.uk; phone: (0044)-
17 141-548-3725

18

19 **Abstract**

20 Parasitic worms are receiving much attention as a potential new therapeutic approach
21 to treating autoimmune and allergic conditions but concerns remain regarding their
22 safety. As an alternative strategy, we have focused on the use of defined parasitic worm
23 products and recently taken this one step further by designing drug-like small molecule
24 analogues of one such product, ES-62, which is anti-inflammatory by virtue of covalently
25 attached phosphorylcholine moieties. Previously, we have shown that ES-62 mimics
26 are efficacious in protecting against disease in mouse models of rheumatoid arthritis,
27 systemic lupus erythematosus and skin and lung allergy. Given the potential role of
28 chronic inflammation in fibrosis, in the present study we have focused our attention on
29 lung fibrosis, a debilitating condition for which there is no cure and which in spite of
30 treatment slowly gets worse over time. Two mouse models of fibrosis - bleomycin-
31 induced and LPS-induced - in which roles for inflammation have been implicated were
32 adopted. Four ES-62 analogues were tested – **11a** and **12b**, previously shown to be
33 active in mouse models of allergic and autoimmune disease and **16b** and **AIK-29/62**
34 both of which are structurally related to **11a**. All four compounds were found to
35 significantly reduce disease development in both fibrosis models, as shown by
36 histopathological analysis of lung tissue, indicating their potential as treatments for this
37 condition.

38

39 Keywords: drug development; fibrosis; ES-62; immunomodulation; parasitic worm

40

41 Abbreviations: ECM – extracellular matrix; PC – phosphorylcholine; SMA – small
42 molecule analogue

43

44

45 **1. Introduction**

46 During the last few decades, a striking increase in the incidence of allergic and
47 autoimmune conditions has been noted in urban areas of the world (reviewed by Bach,
48 2002). One hypothesis put forward to explain this is that decreased exposure to
49 pathogens via for example, increased hygiene, use of antibiotics and vaccination, has
50 resulted in the human immune system no longer being exposed to a range of
51 organisms, which would normally impact on its development and regulation (the
52 “Hygiene Hypothesis”) (Strachan, 1989). Amongst these organisms, particular attention
53 has been paid to parasitic worms, as examples of inverse correlations observed
54 between the incidence of worm infection and conditions like rheumatoid arthritis (Panda
55 et al., 2013; Panda and Das, 2016) and systemic lupus erythematosus (Panda and Das,
56 2016) are strongly supportive of a role for worms in protection against certain
57 autoimmune conditions. The situation with respect to allergic conditions like asthma
58 does not appear as clear-cut, with parameters such as species of worm parasite,
59 parasite load and age of patient likely to play a role (reviewed by Santiago and Nutman,
60 2016). Nevertheless, mouse model studies of allergy reveal that a wide range of worm
61 species, extracts of worms and defined individual worm products can protect against the
62 development of disease (reviewed by Rzepecka and Harnett, 2014).

63 One particularly well-characterised worm product is ES-62, a secreted protein of the
64 filarial nematode *Acanthocheilonema viteae*, which has anti-inflammatory properties by
65 virtue of covalently attached phosphorylcholine (PC) residues (reviewed by Pineda et
66 al., 2014). ES-62 is able to protect mice against ovalbumin-induced airway
67 hypersensitivity in both acute (Melendez et al., 2007; Rzepecka et al., 2013) and
68 chronic (Coltherd et al., 2016) models of airway hypersensitivity and protection in the
69 chronic model is associated with reduction of airway remodeling. Pathological tissue
70 remodeling is also a feature of fibrosis (reviewed by Duffield et al., 2013), a condition in
71 which repetitive damage of tissue by some form of irritant results in dysregulation of the
72 normal wound-healing response leading to deposition of extracellular matrix (ECM) and
73 remodeled tissue. The previously characterized protective effects of ES-62 against

74 airway remodeling in the chronic ovalbumin-induced hypersensitivity model argue for
75 assessment of its therapeutic potential against lung fibrosis. However, as a large,
76 “foreign” protein it is potentially immunogenic and may have delivery-related issues.
77 Hence, as an alternative approach we have generated a library of drug-like ES-62 small
78 molecule analogues (SMAs) based around its active PC moiety (Al-Riyami et al., 2013).
79 Our recent studies have investigated three SMAs termed **11a**, **12b** and **19o**. The first
80 two compounds, like ES-62, are able to inhibit proinflammatory cytokine production by
81 macrophages (Al-Riyami et al., 2013) and are protective in acute (Rzepecka et al.,
82 2015a) and chronic (Coltherd et al., 2016) models of ovalbumin-induced airway
83 hypersensitivity. Conversely **19o** was found to have no effect on macrophage cytokine
84 production (Al-Riyami et al., 2013) and although it has not been tested in the asthma
85 models, it was found, unlike **11a** and **12b**, to be unable to prevent spontaneous kidney
86 disease development in the MRL/lpr mouse model of systemic lupus erythematosus
87 (Rodgers et al., 2015). Our examinations to date indicate that active SMAs like 11a and
88 12b mimic a primary ES-62 mechanism of action in causing autophagolysosomal
89 degradation of the TLR/IL-1R adaptor molecule MyD88 (Al-Riyami et al, 2013;
90 Rzepecka et al, 2015b; Rodgers et al. 2015). Indeed, recently we have found that this
91 reflects direct interaction between the SMAs and the TIR domain of MyD88 (Suckling et
92 al. 2018).

93
94 The aim of this study was thus to test the two active SMAs – **11a** and **12b** - and also
95 two further structurally-related SMAs, **16b** and **AIK-29/62**, against development of
96 pulmonary fibrosis in two distinct mouse models – LPS and bleomycin-induced fibrosis.
97 Bleomycin is a cytostatic drug and a chemotherapeutic antibiotic produced by the
98 bacterium “*Streptomyces verticillus*” that is commonly employed in the treatment of
99 cancer. As a side effect of its therapeutic use, repeated systemic administration of
100 bleomycin induces chronic pulmonary inflammation in some patients that may progress
101 to fibrosis (Moeller et al., 2008). Bleomycin causes injury which follows a pattern of
102 acute neutrophilic inflammation and disruption of the alveolar capillary barrier that
103 usually peaks between days 3–7, followed by resolution of inflammation and

104 development of a fibroproliferative phase. Bleomycin-induced pulmonary fibrosis is a
105 well-established disease model for idiopathic pulmonary fibrosis and widely used in the
106 investigation of therapeutic molecules. LPS, an endotoxin of Gram-negative bacteria is
107 known to cause acute lung injury (ALI). LPS exerts its biological effects through Toll-like
108 receptor 4 (TLR4) and promotes secretion of pro-fibrotic cytokines, including
109 transforming growth factor- β 1 (TGF- β 1). LPS stimulation eventually results in the
110 deposition of extracellular matrix (ECM): of note, therefore, we have previously found
111 two of the ES-62 SMAs employed in the current study, **11a** and **12b**, to interfere with
112 LPS-induced pro-inflammatory responses (e.g. cytokine production) by macrophages
113 (Al-Riyami et al., 2013) and dendritic cells (Lumb et al., 2017) *in vitro*.

114

115

116

117 **2. Materials & Methods**

118 **2.1 Experimental Animals**

119 Female C57BL/6 mice (10-11 week old), with body weight range of 17-21 grams were
120 procured from Charles River (USA). Animals were housed under standard specific
121 pathogen-free conditions in vented cages. Experiments were conducted according to
122 protocols approved by IAEC (Institutional Animal Ethics Committee), IAEC/JDC/2014/54
123 at Jubilant Biosys, with mice acclimatized to these conditions for two weeks prior to
124 dosing. Mice were randomized based on body weight, into groups (n=5/6 per group)
125 such that mean body weights of animals in different groups were not statistically
126 significant and variations within a group spanned less than 20%.

127

128 **2.2 Chemicals**

129 Bleomycin sulphate was purchased from Alfa Aesar (J60727); LPS (*E. coli* serotype
130 055:B5; L2880), dexamethasone (dimethyl sulfoxide (DMSO) soluble), pepsin, DMSO,
131 bovine serum albumin (BSA) and phosphate buffered saline (PBS) were purchased
132 from Sigma. Bleomycin sulphate (50 µg per mouse) and LPS (40 µg per mouse) were
133 prepared by dissolving in PBS immediately prior to use. ES-62 SMAs used in this
134 investigation were **11a**, **12b**, **16b** and **AIK-29/62** and each was synthesised at the
135 University of Strathclyde. **11a**, **12b**, and **16b** have been described and employed
136 previously (Al-Riyami et al., 2013; Rzepecka et al., 2015a); **AIK-29/62** is a new
137 compound (Fig. 1). The main stocks (100 mg/ml) were prepared in DMSO (D2650,
138 Sigma) and stored at -80°C. The SMA sub-stocks (1 mg/ml) were prepared in DMSO
139 and were stored in 4°C until use. At the time of the experiments, the SMAs were diluted
140 1:200 with PBS and a dose volume of 200 µl injected subcutaneously on the scruff of
141 the neck. The same DMSO concentration (0.5%) was maintained in the control PBS
142 (“Vehicle”) group. Dexamethasone 0.4 mg/kg was prepared in PBS and injected by the
143 intra-peritoneal route, as an internal disease protection control.

144

145

146 **2.3 Sirius red Collagen assay**

147 The Sirius Red Collagen Detection Kit (catalog no. 9062) was purchased from
148 Chondrex Inc, USA) and the assay was performed as per manufacturer's instructions.
149 Briefly, the left lobe of the lung (superior & inferior left lobe) was collected and flash
150 frozen immediately in a sterile pre-weighed 1.5 ml Eppendorf tube containing 2 metal
151 beads of 4 mm thickness and stored at -80°C until processed. For processing the
152 samples, 300 µl of milli-Q water was added to promote lysis. Tissue lysis was performed
153 on a pre-chilled metal block in a Geno grinder (Geno / Grinder® SPEX Sample Prep P
154 2010) at 900 rpm for 2 min for 4 cycles. Pepsin (100 µl; from porcine gastric mucosa,
155 P7000, Sigma) prepared as 1 mg/ml in 0.05 M acetic acid (supplied in Chondrex Kit)
156 was added to each sample tube. The contents were gently mixed and incubated
157 overnight at 4°C in an end-to-end rotor, with ~20 µl of sample removed for protein
158 estimation using the Bradford reagent from Biorad. The following day samples were
159 centrifuged at 8,000 rpm for 10 min before transfer of 250 µl of the clear supernatant
160 into a clear 1.5 ml Eppendorf tube. Sirius Red solution (500 µl) was added to the
161 supernatant, and the sample vortexed and incubated overnight at 4°C. Collagen
162 standards (starting conc. of 500 µg/ml) were prepared in 0.05% acetic acid as per
163 manufacturer's instructions, with 100 µl of standard solutions transferred into fresh
164 tubes. Sirius Red solution (500 µl) was added to all the standard tubes, which were then
165 vortexed and incubated overnight at 4°C. The next day standards and samples were
166 centrifuged at 10,000 rpm for 25 minutes at 4°C and the supernatant discarded carefully
167 without disturbing the pellet. The pellet was washed twice using 500 µl of wash solution
168 before addition of 250 µl of extraction buffer and vortexing to completely dissolve the
169 pellet. Samples (200 µl) were transferred to a 96-well plate, and the OD read at 510-550
170 nm.

171 **2.4 Histopathological evaluation**

172 Mouse lung (right inferior lobe) tissues were processed for routine paraffin embedding
173 and serial sections of 6 µm thickness were prepared. Slides were stained with
174 hematoxylin and eosin (H & E) for detailed examination of tissue pathology whilst the

175 Richard Allan Gomori Trichrome staining kit (Thermo Scientific) was employed to
176 assess the collagen content, visualised as blue fibers. The extent of disease severity
177 was assessed using the modified Ashcroft scale (Hubmer et al., 2008) where the entire
178 lung section was examined for pulmonary fibrotic changes and sections representative
179 of the scoring system are shown in Fig. 2. This clinical scoring reflects the extent and
180 severity of cellularity in the alveolar wall (interstitium); metaplastic cells lining the air
181 spaces, including foci of honeycomb lung; the extent and severity of cellularity in the
182 alveolar space (desquamation); interstitial “young connective tissue” interstitial fibrosis;
183 honeycomb cysts; metaplastic smooth muscle in the stroma; myointimal mural
184 thickening in the vessel walls; airway luminal granulation tissue; air space granulation
185 tissue; airway wall inflammation; airway wall fibrosis, as indicated.

186

187 **2.5 Study Protocol**

188 This study comprised two arms, with the objectives being the investigation of bleomycin-
189 and LPS-induced lung fibrotic changes. 70 animals were procured and randomized
190 based on the study plan. Pulmonary fibrosis was induced either by a single dose of
191 oropharyngeal instillation with 50 µg bleomycin sulphate (dissolved in 40 µl of PBS) or
192 40 µg of LPS (dissolved in 40 µl of PBS). Mice that were injected with PBS served as
193 controls. The four test compounds were dosed at 0.05 mg/kg and dexamethasone at
194 0.4 mg/kg. Animals from respective treatment groups were administered with vehicle or
195 test compound/dexamethasone for 6 days a week and dexamethasone thrice weekly
196 starting from day 0 to 7 for the LPS group and day 0 to 13 for the bleomycin group.
197 Mortality (if any), clinical signs, and body weight (3-4 days weekly) were recorded. The
198 animals were sacrificed on day 8 (LPS group) or day 14 (bleomycin group), time-points
199 chosen on the basis of our previous experiments analysing collagen deposition. Lung
200 lobes were sampled according to the relevant assays (left lung lobes: superior and
201 inferior for collagen assay; right superior and middle lobe as reserve and right inferior
202 lobe for histopathology analysis) and tissue weights were recorded. Lung lobes were
203 analyzed for collagen levels and histopathological analysis. One mouse from the

204 bleomycin-treated cohort was found dead on Day 12, presumably due to disease
205 severity. One animal each from dexamethasone-treated (bleomycin-induced) and AIK-
206 29/62 treated (LPS-induced) groups were found dead on the day of sensitization (day
207 0), presumably due to the challenges in recovery from anesthesia.

208

209

210 **2.6 Statistical Analysis**

211 All statistical analyses were performed using Graphpad Prism software, using a one-
212 way ANOVA or 2-way ANOVA analysis and Fisher's least significance difference post-
213 test or Kruskal Wallis post-test where stated for the Ordinal Histopathology data.

214

215

216

217 **3. Results**

218 ***3.1 Histopathological assessment of effect of ES-62 SMAs in models of lung***
219 ***fibrosis***

220 Histopathological analysis of lung tissues revealed that lung parenchyma of LPS and
221 bleomycin disease groups display significant pathology with development of alveolar
222 septa, widening and disturbance of alveolar structure, severe inflammatory cell
223 infiltration, and excessive collagen deposition. By contrast, mice treated with **11a**, **12b**,
224 **16b**, **AIK-29/62** or dexamethasone showed substantial protection from LPS- and
225 bleomycin-induced damage such as reduction in each of alveolar septa widening,
226 inflammatory cell infiltration, fibroblast proliferation and excessive collagen deposition
227 (Fig. 3A). Supporting this, the scoring of disease severity showed that whilst both the
228 LPS- and Bleomycin-disease groups have scores significantly different to those of the
229 vehicle mice, none of the treated groups (**11a**, **12b**, **16b**, **AIK-29/62** or dexamethasone)
230 displayed scores significantly different from the healthy mice (Fig. 3B).

231

232 ***3.2 Effect of ES-62 SMAs on body weight and lung tissue weight in models of***
233 ***fibrosis***

234 Following an initial drop in body weight following treatment with LPS, the animals
235 generally recovered over the duration of the experiment and ultimately, the administered
236 compounds had little effect on the weight of the animals (Fig. 4). Treatment with
237 bleomycin showed some evidence of causing a reduction in body weight although this
238 did not reach statistical significance. Relative to the no disease control group, all of the
239 LPS-treatment groups showed slightly elevated dry lung weights, which were not
240 significantly decreased by any of the interventions, although those treated with AIK-
241 29/62 or dexamethasone were not significantly different from healthy controls. The lung
242 tissue weights of diseased animals in the bleomycin groups treated with PBS, 11a or
243 12b were also significantly higher when compared to the control group whereas
244 treatment with each of SMA **16b** and **AIK-29/62** suppressed this (Fig. 5). Indeed, the
245 lung weights of these two treatment groups and in addition dexamethasone were not
246 significantly different from healthy controls.

247

248 **3.3. Effect of ES-62 SMAs on collagen deposition in models of fibrosis**

249 Fibrosis results from an abnormal wound-healing response following alveolar injury
250 forming a scar. The fibroblasts involved in scarring have a myofibroblast phenotype
251 characterized by α -smooth muscle actin (α -SMA) expression and increased secretion of
252 collagen types I and III. The collagen content in fibrotic tissues was estimated using
253 Sirius Red dye, which specifically binds to the [Gly-X-Y]_n helical structure on fibrillar
254 collagen (type I to V) but does not discriminate between collagen species and types.

255 Collagen levels were estimated from the left superior and inferior lobes of mice and
256 expressed as micrograms of collagen per milligram tissue ($\mu\text{g}/\text{mg}$). LPS and bleomycin
257 both significantly increased the levels of collagen detected: administration of 0.05 mg/kg
258 of compound **AIK-29/62** or dexamethasone attenuated collagen deposition in the LPS-
259 treated mice as shown by statistically significant differences from the LPS-PBS control
260 (Fig. 6). The other treatments had no statistically significant effect and likewise, none of
261 the treatments were able to prevent bleomycin-induced collagen deposition.

262

263

264 4. Discussion

265

266 Fibrosis, or scarring, is defined by the accumulation of excess extracellular matrix
267 (ECM) components such as collagen and fibronectin in and around the inflamed or
268 damaged area which can further lead to permanent scarring, organ malfunction and
269 ultimately death (reviewed by Duffield et al., 2013). In this study, we investigated the
270 protective effects of synthetic SMAs of the immunomodulatory parasitic worm product
271 ES-62 against fibrosis. These SMAs are drug-like compounds that have previously been
272 shown to protect against inflammatory exacerbations in an ovalbumin-dependent model
273 of chronic asthma (Coltherd et al., 2016).

274

275 As expected, both bleomycin and LPS caused fibrosis to develop in the lungs of treated
276 mice. SMAs **11a** and **12b**, when tested in quantities analogous to those previously
277 shown to protect against disease development in models of allergy and autoimmunity
278 (Al-Riyami et al., 2013; Rzepecka et al., 2015a; Rzepecka et al., 2015b), were able to
279 significantly reduce this and to a level comparable to the disease-active control
280 compound, dexamethasone. The two compounds new to *in vivo* evaluation, SMAs **16b**
281 and **AIK-29/62**, are structurally related to SMA **11a** and they too behaved in a similar
282 manner to dexamethasone when tested in the model. **12b** is rather different in chemical
283 structure, being the only one of the four SMAs evaluated that can readily form a vinyl
284 sulfone. As we discussed previously (Rzepecka et al., 2015b), because a vinyl sulfone
285 has potential for additional biological activity to that related to ES-62 it is possible that
286 this could contribute to the observed behavior of **12b** in not reducing collagen
287 deposition. In any case, all four compounds showed therapeutic potential for the
288 treatment of fibrosis. Caution should be observed with respect to **AIK-29/62** as there is
289 some indication that it may be enhancing the reduction in body weight observed when
290 employing bleomycin, although this was not statistically significant by the end of the
291 experiment. At the same time, however, SMAs **AIK-29/62** and **16b** were able to
292 significantly inhibit the observed increase in lung tissue weights observed in bleomycin-
293 treated groups.

294

295 To investigate their mechanism of action, we also measured the amount of collagen
296 present in the lungs: whilst both LPS and bleomycin significantly increased collagen
297 levels, only SMA **AIK-29/62** and dexamethasone were able to significantly prevent this
298 and only with respect to LPS treatment. Relating to this general absence of an effect
299 with the SMAs, we had previously subjected **12b**-exposed bone marrow-derived
300 macrophages to microarray analysis (Rzepecka et al. 2015b) and noted no effect on
301 expression of collagen genes such as col1a2 and col3a1. At the same time however, 9
302 of the genes present in the mouse fibrosis PCR array produced by Quiagen were
303 affected. In eight of these cases the change was in a direction likely to inhibit fibrosis.
304 Thus, there is decreased expression of the genes corresponding to 6 mediators that
305 play a role in pulmonary fibrosis – CCR2 (Moore et al. 2001) – expression reduced 3.8-
306 fold; IL-1 β (Borthwick, 2016) – expression reduced 8.9-fold (most affected gene in the
307 study); PDGFB (Abdollahi *et al.*, 2005) – expression reduced 2.1-fold; TGFB1
308 Fernandez and Eickelberg, 2012) – expression reduced 1.6-fold; TGFB3 (Emblom-
309 Callahan et al., 2010) – expression reduced 2.1-fold and NF κ B1 (Christman, Sadikot
310 and Blackwell, 2000) – expression reduced 1.8-fold. At the same time, there is
311 increased expression (2.9-fold) of Mmp13, an enzyme found to limit the overall
312 magnitude of ECM build up in the fibrotic lung (Nkyimbeng et al., 2013) and uPa (2.6-
313 fold), which would be expected to result in increased collagen degradation and tissue
314 fibrogenesis (Ghosh and Vaughan, 2012) The only gene that showed a change in
315 expression that is perhaps more difficult to reconcile with a protective role against
316 fibrosis is CCL3 L1/L3 (1.7-fold increase) as the chemokine CCL3 is considered to play
317 a role in promoting fibrosis (Yang et al. 2011). Overall however, the changes in gene
318 expression are clearly consistent with a protective effect against fibrosis and thus mirror
319 the protective effects shown in the present study.

320

321 In summary, parasitic worm products are increasingly being considered as novel
322 therapeutics for human illnesses associated with aberrant inflammatory responses
323 (reviewed by Rzepecka and Harnett, 2014). We have recently taken this a step further

324 via the production of synthetic drug-like SMAs of one of the best characterized of these
325 molecules, ES-62 (Al-Riyami et al., 2013). In the current study, we demonstrate that
326 these SMAs are effective in modulating key efficacy markers in a subset of fibrotic
327 diseases. Potentially, these offer a novel approach to the treatment of fibrosis, a
328 debilitating condition for which current therapies remain inadequate. With respect to
329 obtaining a candidate drug based upon these and cited results, SMAs **11a** and **12b** do
330 not have hERG or CYP inhibition liabilities but optimization will be required in terms of
331 pharmacokinetic properties and dosing regime, for the treatment of fibrosis or other
332 appropriate diseases.

333

334

335 **Funding:** This research did not receive any specific grant from funding agencies in the
336 public, commercial, or not-for-profit sectors.

337 **5. References**

338

339 Abdollahi, A. et al. (2005) Inhibition of platelet derived growth factor signaling attenuates
340 pulmonary fibrosis. *Journal of Experimental Medicine* 201, 925-935.

341 Al-Riyami, L., Pineda, M.A., Rzepecka, J., Huggan, J.K., Khalf, A.I., Suckling, C.J.,
342 Scott, F.J., Rodgers, D.T., Harnett, M.M. and Harnett, W. (2013) Designing anti-
343 inflammatory drugs from parasitic worms: a synthetic small molecule analogues of the
344 *Acanthocheilonema viteae* product ES-62 prevents development of collagen-induced
345 arthritis. *Journal of Medicinal Chemistry* 56, 9,982-10,002.

346 Bach, J.F. (2002) The effect of infections on susceptibility to autoimmune and allergic
347 diseases. *New England Journal of Medicine* 347, 911-920.

348 Borthwick, L.A. (2016) The IL-1 cytokine family and its role in inflammation and fibrosis
349 in the lung. *Semin. Immunopathol.* 38, 517-534.

350 Christman, J.W., Sadikot, R.T. and Blackwell, T.S. (2000) The role of nuclear factor- κ B
351 in inflammatory diseases. *Chest* 117, 1,482-1,487.

352 Coltherd, J.C., Rodgers, D.T., Lawrie, R.E., Al-Riyami, L., Suckling, C.J., Harnett, W.
353 and Harnett, M.M. (2016) The parasitic worm-derived immunomodulator ES-62 and its
354 drug-like small molecule analogues exhibit therapeutic potential in a model of chronic
355 asthma. *Scientific Reports*, January 14, e.publication.

356 Duffield, J.S., Lupper, M., Thannickal, V.J. and Wynn, T.A. (2013) Host responses in
357 tissue repair and fibrosis. *Annual Review of Pathology* 8, 241-276.

358 Emblom-Callahan, M.C. et al. (2010) Genomic phenotype of non-cultured pulmonary
359 fibroblasts in idiopathic pulmonary fibrosis. *Genomics* 96, 134-145.

360 Fernandez, I.E. Eickelberg, O. (2012) The impact of TGF- β on lung fibrosis. *Proc. Am.*
361 *Thorac. Soc.* 9, 111-116.

362 Ghosh, A.K and Vaughan, D.E. (2012) PAI-1 in tissue fibrosis. *J Cell. Physiol.* 227, 493-
363 507.

364 Hubner, R.H., Gitter, W., El Mohktari, N.E., Mathiak, M., Both, M., Bolte, H., Freitag-
365 Wolf, S. and Bewig, B. (2008) Standardised quantification of pulmonary fibrosis in
366 histological samples. *Biotechniques* 44, 507-511.

367 Lumb, F.E., Doonan, J., Bell, K.S., Pineda, M.A., Corbet, M., Suckling, C.J., Harnett,
368 M.M. and Harnett, W. (2017) Dendritic cells provide a therapeutic target for synthetic
369 small molecule analogues of the parasitic worm product, ES-62. *Scientific Reports*, May
370 10, e.publication.

371 Melendez, A.J., Harnett, M.M., Pushparaj, P.N., Wong, W.S., Tay, H.K., McSharry, C.P.
372 and Harnett, W. (2007) Inhibition of FcεRI-mediated mast cell responses by ES-62: a
373 product of parasitic filarial nematodes. *Nature Medicine* 13: 1,375-1,381.

374 Moeller, A., Ask, K., Warburton, D., Gauldie, J. and Kolb, M. (2008) The bleomycin
375 animal model: a useful tool to investigate treatment options for idiopathic pulmonary
376 fibrosis? *International Journal of Biochemistry and Cell Biology* 40, 362-382.

377 Moore, B.B., Paine III, R., Christensen, P.J., Moore, T.A., Sitterding, S., Ngan, R.,
378 Wilkie, C.A., Kuziel, W.A. and Toews, G.B. (2001) Protection from pulmonary fibrosis in
379 the absence of CCR2 signaling. *Journal of Immunology* 167, 4,368-4,377.

380 Nkyimebeng, T. et al. (2013) Pivotal role of matrix metalloproteinase 13 in extracellular
381 matrix turnover in idiopathic pulmonary fibrosis. *PLOS One*, e73279.

382 Panda, A.K. and Das, P.K. (2016) diminished IL-17A levels may protect filarial-infected
383 individuals from development of rheumatoid arthritis and systemic lupus erythematosus.
384 *Lupus*, August 3, e.publication.

385 Panda, A.K., Ravindran, B. and Das, B.K. (2013) Rheumatoid arthritis patients are free
386 of filarial infection in an area where filariasis is endemic: comment on the article by
387 Pineda et al. *Arthritis and Rheumatism* 64, 1,402-1,403.

388 Pineda, M.A., Lumb, F., Harnett, M.M. and Harnett, W. (2014) ES-62, a therapeutic anti-
389 inflammatory agent evolved by the filarial nematode *Acanthocheilonema viteae*.
390 *Molecular and Biochemical Parasitology* 194: 1-8.

391 Rodgers, D.T., Pineda, M.A., Suckling, C.J., Harnett, W. and Harnett, M.M. (2015)
392 Drug-like analogues of the parasitic worm-derived immunomodulator ES-62 are
393 therapeutic in the MRL/lpr model of systemic lupus erythematosus. *Lupus* 24, 1437-
394 1442.

395 Rzepecka, J., Coates, M.L., Saggar, M., Al-Riyami, L., Coltherd, J., Tay, H.K., Huggan,
396 J.K., Janicova, L., Khalaf, A.I., Siebeke, I., Suckling, C.J., Harnett, M.M. and Harnett, W.
397 (2015a) Small molecule analogues of the immunomodulatory parasitic helminth product
398 have anti-allergy properties. *International Journal for Parasitology* 44, 669-674.

399 Rzepecka, J. and Harnett, W. (2014) Can the study of helminths be fruitful for human
400 diseases? In: *Helminth infections and their impact on global public health*". Ed: Bruschi,
401 F. Springer, Wein. pp. 479-502.

402 Rzepecka, J., Pineda, M.A., Al-Riyami, L., Rodgers, D.T., Huggan, J.K., Lumb, F.E.,
403 Khalaf, A.I., Meakin, P.J., Corbet, M., Ashford, M.L., Suckling, C.J., Harnett, M.M. and
404 Harnett, W. (2015b) Prophylactic and therapeutic treatment with a synthetic analogue of
405 a parasitic worm product prevents experimental arthritis and inhibits IL-1b production via
406 NRF2-mediated counter-regulation of the inflammasome. *Journal of Autoimmunity* 60,
407 59-73.

408 Rzepecka, J., Siebeke, I., Cotlherd, J.C., Kean, D.E., Steiger, C.N., Al-Riyami, L.,
409 McSharry, C. P., Harnett, M.M. and Harnett, W. (2013) The helminth product ES-62
410 protects against airway inflammation by resetting the Th cell phenotype. *International*
411 *Journal for Parasitology* 43: 211-223.

412 Santiago, H.C. and Nutman, T.B. (2016) Human helminths and allergic disease: the
413 hygiene hypothesis and beyond. *American Journal of Tropical Medicine and Hygiene*
414 95, 746-753.

415 Strachan, D.P. (1989) Hay fever, hygiene and household size. *British Medical Journal*
416 299, 1,259-1,260.

417 Suckling, C.J., Alam, S., Olson, M.A., Saikh, K.U., Harnett, M.M. and Harnett, W. (2018)
418 Small molecule analogues of the parasitic worm product ES-62 interact with the TIR
419 domain of MyD88 to inhibit proinflammatory signaling. *Scientific Reports*, 8(1):2123.

420 Yang, X. et al. (2010) The chemokine, CCL3, and its receptor, CCR1, mediate thoracic
421 radiation-induced pulmonary fibrosis. *Am. J. Respir. Cell. Mol. Biol.* 45, 127-135.

422

423

424 **Figure Legends**

425

426 **Fig. 1. Structures and properties of the ES-62 SMAs.**

427

428 **Fig. 2. Representative images of the clinical scoring of fibrosis from LPS and**
429 **Bleomycin treated groups.** Lung histology shows H & E staining (left panels; 10X
430 magnification) and Trichrome Gomori staining (right panels; 10X magnification; collagen
431 is stained in blue). Scores 0, 1, 2, 3, 5 and 6 represent increases in disease severity.
432 Slides with a score of 0, 3, and 5 are from the LPS-treated group, whilst those with a
433 score of 1, 2, and 6 are from the Bleomycin treatment group. In this study, we did not
434 find tissue exhibiting a score representative of 4.

435

436 **Fig. 3. Protection against fibrosis by SMAS 11a, 12b, 61 and AIK-29/62. A.** Lung
437 histology shows 2 representative images of Trichrome Gomori (10X magnification)
438 staining of the lungs from each group. Excessive collagen deposition and inflammatory
439 cell infiltration were visible in the disease groups. **B.** Lung histopathological scores of
440 the groups where data are represented as mean \pm SEM (n=5 LPS [except 62, n=4]; n=6
441 bleomycin [except PBS n=5 and dexamethasone (Dex) n=4]). Analysis by 1-way
442 ANOVA and Kruskal Wallis post-test showed that LPS and bleomycin induce significant
443 increases (*p<0.05; **p<0.001) in disease severity compared to the no-disease control
444 group (Vehicle) and #, ## denotes the significant decrease (#p<0.05, ##p<0.01) in
445 disease severity resulting from treatment with the SMAs compared to the disease
446 control (PBS) group. AIK-29/62 is denoted by "62". None of the animals treated with the
447 SMAs or dexamethasone showed scores significantly different to the healthy control
448 cohort.

449

450 **Fig. 4: Body weight representation from LPS (A) and Bleomycin (B) groups.** Data
451 are presented as mean \pm SEM (n=5 for LPS groups, except for “62” group n=4; n=6 for
452 bleomycin groups, except for PBS group n=5 and for Dex group n=4). Data were
453 analysed by 2-way ANOVA.

454 For LPS:

455 Day 1: ***p<0.001 for LPS + PBS, LPS + **11a**, LPS + **12b**, LPS + **16b**; **p<0.01 for LPS
456 + **AIK-29/62** (denoted by “62”) and *p<0.05 for LPS + Dex, all versus Vehicle, i.e., no
457 LPS-induced disease

458 Day 3: **p<0.01 for LPS + PBS and *p<0.05 for LPS + **11a**, LPS + **12b**, LPS + **16b**, all
459 versus Vehicle

460 Day 8: *p<0.05 for LPS + PBS and LPS + Dex, versus Vehicle

461 For bleomycin

462 Day1: *p<0.05 for bleomycin + **16b** and bleomycin + **AIK-29/62** (denoted by “62”).
463 versus Vehicle, i.e., no bleomycin-induced disease

464 Day 3: *p<0.05 for bleomycin + **AIK-29/62** (denoted by “62”) versus Vehicle

465 Day 6: *p<0.05 for bleomycin + **AIK-29/62** (denoted by “62”) versus Vehicle)

466 Day 8: *p<0.05 for bleomycin + PBS, bleomycin + **11a**, bleomycin + **12b**, bleomycin + Dex
467 and ***p<0.001 for bleomycin + **AIK-29/62** (denoted by “62”) versus Vehicle

468

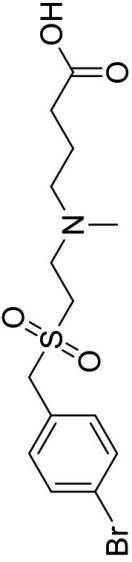
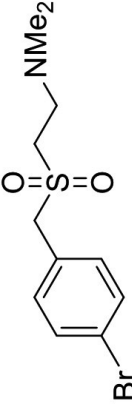
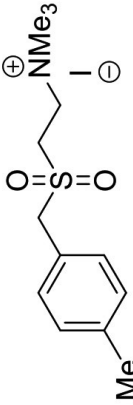
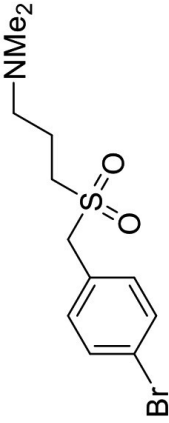
469 **Fig. 5: Tissue weights of left lung lobe from LPS- and bleomycin-groups.** Data are
470 represented as mean \pm SEM (n=5 LPS, except for **AIK-29/62** [denoted by “62”, n=4] as
471 one-treated mouse died on d1; n=6 bleomycin, except for PBS=5 as one mouse died on
472 d13 and for Dex =4 as one mouse died on d1). Significant increases (*p<0.05; **p<0.01
473 and ***p<0.001) in tissue weight compared to Vehicle are indicated whilst suppression
474 of LPS- or bleomycin responses by treatments are denoted by #p<0.05 as analysed by
475 1-way ANOVA.

476

477 **Fig. 6: Analysis of collagen concentration per left lung lobe from cohorts of LPS-**
478 **and bleomycin-induced fibrosis, represented in μg per mg of lung tissue.** Data are
479 represented as mean \pm SEM (n=5 LPS, except for **AIK-29/62** [denoted by "62", n=4] as
480 one-treated mouse died on d1; n=6 bleomycin, except for PBS=5 as one mouse died
481 d13 and for Dex =4 as one mouse died d1). Significant increases (*p<0.05; **p<0.01)
482 compared to Vehicle are indicated whilst suppression of LPS- or Bleomycin responses
483 by particular treatments are denoted by #p<0.05 as analysed by 1-way ANOVA.

484

485

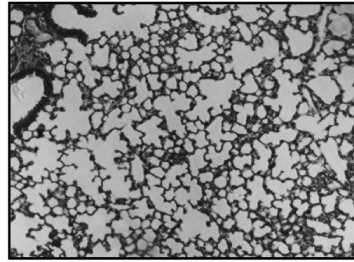
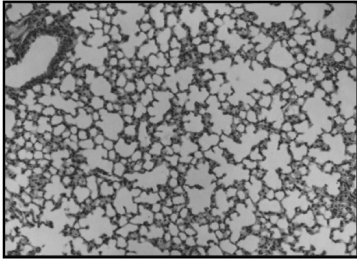
Code	Structure	MW/Formula
AIK-29/62		378.28 C ₁₄ H ₂₀ BrNO ₄ S
11a [S3]		305.01 C ₁₁ H ₁₆ BrNO ₂ S
12b [S5]		383.04 C ₁₃ H ₂₂ INO ₂ S
16b		320.25 C ₁₂ H ₁₈ BrNO ₂ S
Prototype PC-ES-62	Protein—Carbohydrate—O—P(=O)(O ⁻)—O—CH ₂ —CH ₂ —NMe ₃ ⁺	

Score

H & E

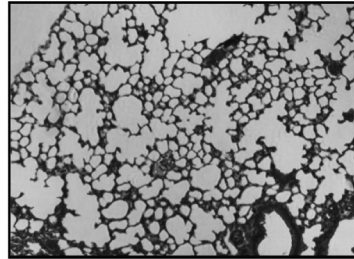
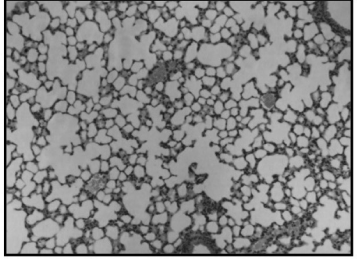
Trichrome Gomori

0



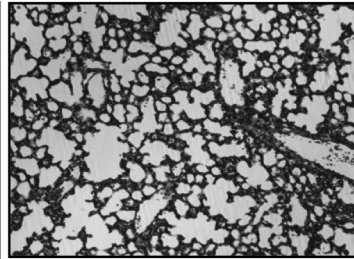
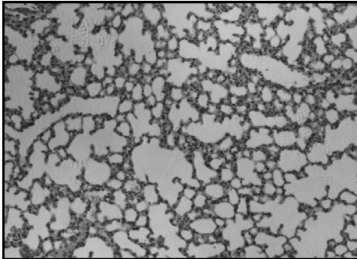
Normal lung

1



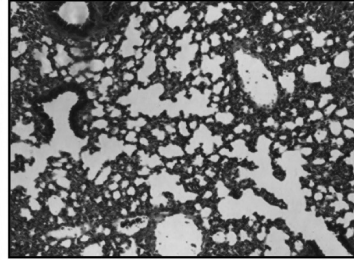
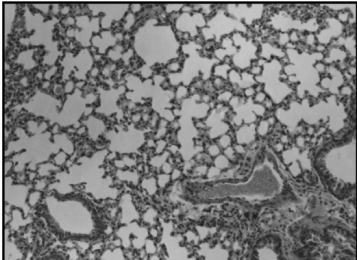
Gentle fibrotic changes,
alveoli partly enlarged

2



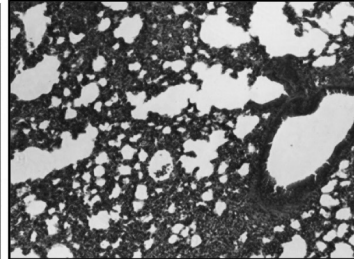
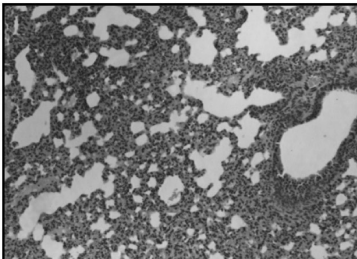
Knot-like formation

3



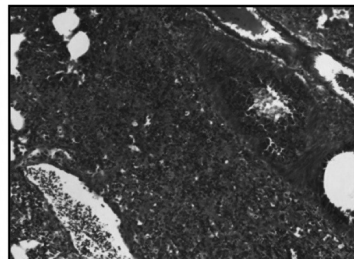
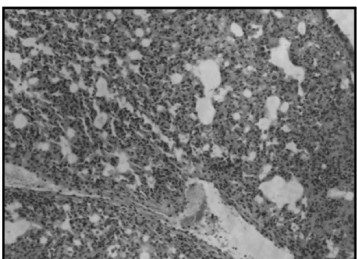
Continuous fibrotic walls,
alveoli partly enlarged

5



Variable alveolar septa,
confluent fibrotic mass,
lung structure damaged in
10-50% of microscopic field

6

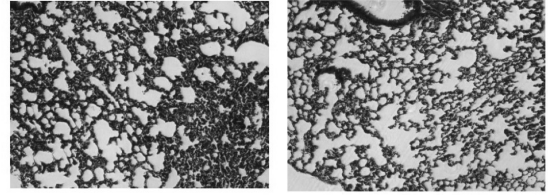
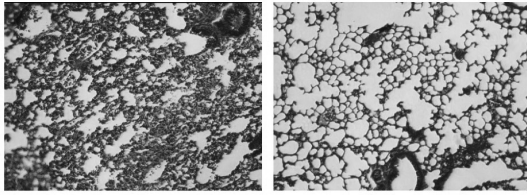


Alveolar septa mostly not
existent, continuous fibrotic
mass in >50% of field

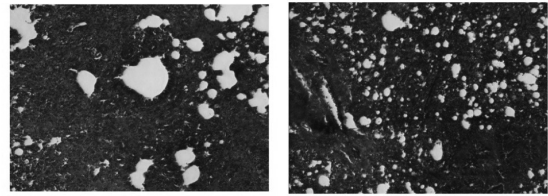
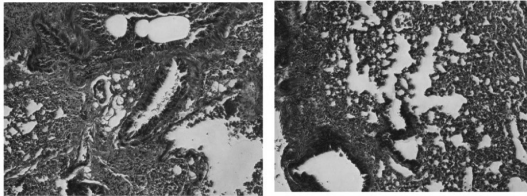
LPS-induced fibrosis

Bleomycin-induced fibrosis

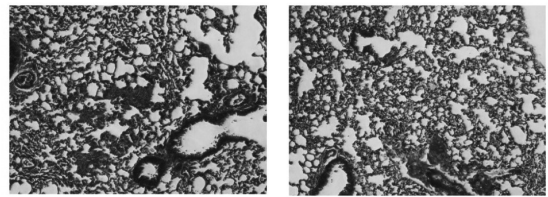
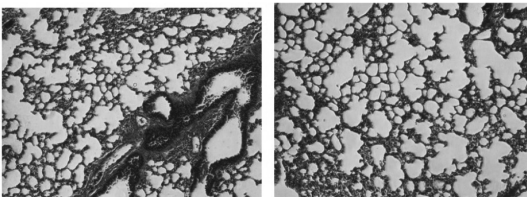
**Vehicle
Healthy
Control**



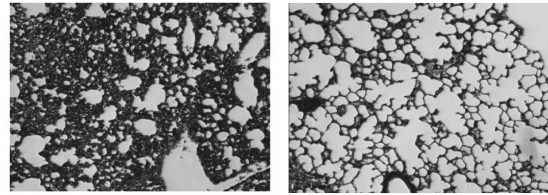
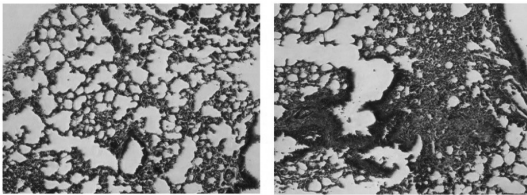
**PBS
Disease
Control**



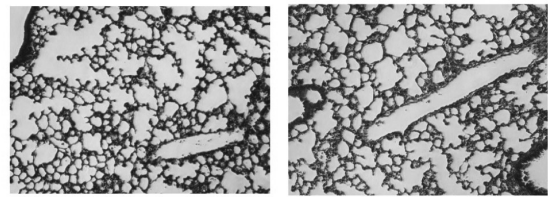
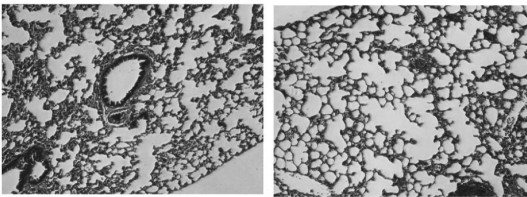
11a



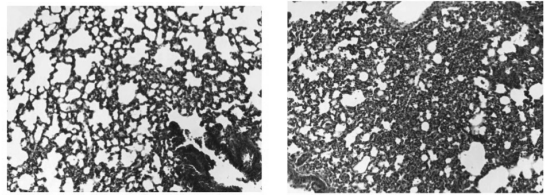
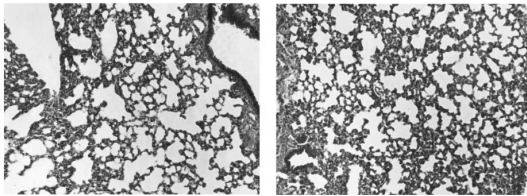
12b



16b



**AIK-29/62
(62)**



Dex

